

# Thermal effect on axisymmetric bending of functionally graded circular and annular plates using DQM

N. Safaeian Hamzehkolaei<sup>1</sup>, P. Malekzadeh<sup>2</sup>, and J. Vaseghi<sup>1\*</sup>

<sup>1</sup>Department of Civil Engineering, Babol University of Technology, P.O. Box 484, Babol, Iran

<sup>2</sup>Department of Mechanical Engineering, Persian Gulf University, Bushehr 75168, Iran

(Received July 11, 2010, Accepted June 22, 2011)

**Abstract:** This paper presents the effects of thermal environment and temperature-dependence of the material properties on axisymmetric bending of functionally graded (FG) circular and annular plates. The material properties are assumed to be temperature-dependent and graded in the thickness direction. In order to accurately evaluate the effect of thermal environment, the initial thermal stresses are obtained by solving the thermoelastic equilibrium equations. Governing equations and the related boundary conditions, which include the effects of initial thermal stresses, are derived using the virtual work principle based on the elasticity theory. The differential quadrature method (DQM) as an efficient and robust numerical tool is used to obtain the initial thermal stresses and response of the plate. Comparison studies with some available results for FG plates are performed. The influences of temperature rise, temperature-dependence of material properties, material graded index and different geometrical parameters are carried out.

**Keywords:** bending analysis; functionally graded; annular plates; elasticity theory; thermal environment.

---

## 1. Introduction

Functionally graded materials (FGMs) are heterogeneous composite materials with gradient compositional variation of the constituent (usually metal and ceramic) along the thickness direction which result in continuously varying material properties.

Circular and annular plates made of functionally graded materials (FGMs) under high-temperature environment have found in many engineering fields that need to be super heat resistant, such as the outer wall and the engine parts of future space-planes, nuclear engineering and reactors. Hence, the investigation of their thermo-mechanical performance is of great interest for engineering design and manufacture.

In comparison with the research on mechanical and thermo-mechanical bending analysis of FG rectangular plates, see for example (Redy and cheng 2001, Qian et al. 2004 and Ferreira et al. 2005) and the related cited references within them, there is only few study for circular and annular plates. Reddy *et al.* (1999) examined the axisym-metric bending of functionally graded circular and annular plates using the first order shear deformation plate theory (FSDT). A general solution to the Mindlin plate problem for arbitrary variation of the consti-tuents was derived in terms of the isotropic Kirchhoff plate solution. Cheng and Batra (2000) used an asymptotic expansion method to analyze three-dimensional thermoelastic

---

\* Corresponding author, Professor, E-mail: [vaseghi@nit.ac.ir](mailto:vaseghi@nit.ac.ir)

deformations of functionally graded elliptic plates, rigidly clamped at the edges. Ma and Wang (2003) investigated the nonlinear bending and post-buckling of a functionally graded circular plate under mechanical and thermal loadings based on the classical plate theory. Ma and Wang (2004) employed the third-order shear deformation plate theory (TPT) to solve the axisymmetric bending and buckling problems of functionally graded circular plates. Relationships between the TPT solutions of axisymmetric bending and buckling of functionally graded circular plates and those of isotropic circular plates based on the classical plate theory (CPT) were presented.

Najafizadeh and Heydari (2004) investigated thermal buckling of circular plates composed of functionally graded material (FGM). Equilibrium and stability equations of a FGM circular plate under thermal loads are derived, based on the 3rd order shear deformation plate theory. The study concludes that higher order shear deformation theory accurately predicts the behavior of functionally graded circular plate, whereas the first order and classical plate theory overestimates buckling temperature. Li *et al.* (2008) presented an analytical solution for the problem of a uniformly loaded FG, transversely isotropic, magneto electro-elastic circular plate with material properties being the exponential functions of the thickness coordinate based on elasticity theory. In another research, Li *et al.* (2008) investigated the analytical elasticity solutions for a transversely isotropic functionally graded circular plate subject to an axisymmetric transverse load and having material constants as power functions. Saidi *et al.* (2009) studied the axisymmetric bending and buckling of perfect functionally graded solid circular plates based on the unconstrained third-order shear deformation plate theory. The solutions for deflections, force and moment resultants and critical buckling loads in bending and buckling analysis of FG circular plates based on the presented theory were given in terms of the corresponding quantities of the homogeneous plates based on the classical plate theory. Saidi and Hasani (2010) studied the thermal buckling analysis of moderate of thick functionally graded annular sector plates. Thermal buckling of functionally graded annular sector plate for two types of thermal loading, uniform temperature rise and gradient through the thickness, are investigated in their studies. Thermal post-buckling behavior of uniform slender FGM beams is investigated by Anand Rao *et al.* (2010). They are using the classical Rayleigh-Ritz formulation and finite element analysis. The Von-Karman strain-displacement relation are used to account for moderately large deflection of FGM beams. In all the aforementioned papers, the effects of temperature-dependence of material properties on thermo-mechanical bending behavior of FG circular and annular plates were not considered. But it is well accepted that the effect of temperature-dependent mechanical properties should be taken into account in order to perform a more accurate analysis (Noda 1991, Malekzadeh 2009 and Malekzadeh *et al.* 2010a).

To the authors' best knowledge, the axisymmetric thermo-mechanical bending analysis of FG circular and annular plates with temperature-dependent material properties is not investigated previously. Hence, this motivates us to consider this problem. The initial thermal stresses are obtained accurately using the thermoelastic equilibrium equations including the out-of-plane effects. The material properties are assumed to be temperature-dependent and graded in the thickness direction, which can vary according to power law distribution. The differential quadrature method (DQM) as a simple and efficient numerical technique (Malekzadeh 2009, Malekzadeh *et al.* 2010a, Bert and Malik 1996, Malekzadeh *et al.* 2010b, Malekzadeh *et al.* 2008) is employed to solve the governing equations. After demonstrating the convergence and accuracy of the method, the effects of different geometrical parameters, uniform and non-uniform temperature rise and temperature-dependence of the material properties on the response of the plates under different boundary conditions are investigated.

## 2. Theoretical formulation

Consider a FG annular plate with the inner radius  $R_i$ , outer radius  $R_o$  and the total thickness  $h$  as shown in Fig. 1. A polar coordinate system  $(r, \theta, z)$  is used on the middle plane of a plate of uniform thickness  $h$ . The displacement components of the plate are denoted as  $u, v,$  and  $w$  in the  $r$ -,  $\theta$ - and  $z$ -directions, respectively.

### 2.1. Temperature-dependent FGMs relations

The material properties are graded in the thickness direction according to the volume fraction power law distribution. The material composition continuously varies such that the top surface of the plate ( $z = h/2$ ) is ceramic-rich whereas the bottom surface of the plate ( $z = -h/2$ ) is metal-rich. Based on the power law distribution, a typical effective material property ‘ $P$ ’ of the FG plate is obtained as

$$P(z, T) = P_m(T) + [P_c(T) - P_m(T)] \left( \frac{2z + h}{2h} \right)^p \quad (1)$$

Where subscripts  $m$  and  $c$  refer to the metal and ceramic constituents, respectively;  $p(\geq 0)$  is the power law index or the material property graded index which takes values greater than or equal to zero; and  $T [=T(z)]$  is the temperature at an arbitrary material point of the plate.

For the FG plate constituents, *i.e.*, ceramic and metal, the material properties are temperature-dependent and a typical property ‘ $G$ ’ of them can be expressed as a function of temperature as Kim (2005)

$$G(T) = G_0(G_{-1}T^{-1} + 1 + G_1T + G_2T^2 + G_3T^3) \quad (2)$$

The coefficients  $G_i$  ( $i = -1, 0, 1, 2, 3$ ) are unique to the constituent materials and cited in Table 1.

### 2.2. Thermal equilibrium analysis

The thermo elastic equilibrium equations for the initial thermal stress evaluation are presented. For this purpose, it is assumed that the plate is stress free at the temperature  $T_0$  and then it operates in a thermal environment with non-uniform temperature rise or uniform temperature rise together with mechanical constraints at its boundaries. These conditions cause some thermal stresses in the plates and

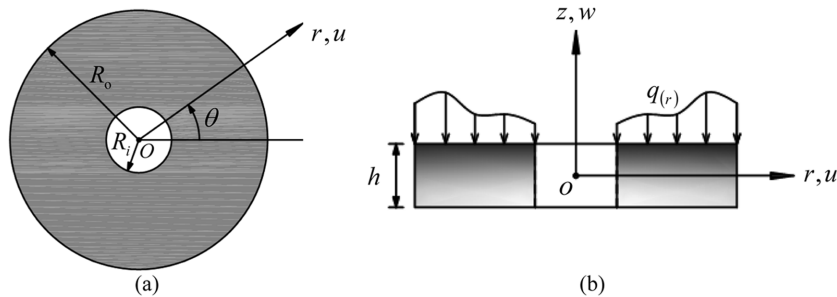


Fig. 1 (a), (b) Geometry and coordinate system of the FG annular plates.

consequently affect the deflection and stresses of the plate under mechanical loading. In this study, the temperature rise is assumed to be uniform or varies across the thickness of the plate and no heat generation source exists within the plate. Hence, the temperature distribution along the thickness direction can be obtained by solving the following steady state one-dimensional heat transfer equation through the thickness of the plate

$$K(z) \frac{d^2 T}{dz^2} + \frac{dK(z)}{dz} \frac{dT}{dz} = 0 \quad (3)$$

where  $K [= K(z)]$  is the thermal conductivity of the plate. Different thermal boundary conditions can be considered at the top and the bottom surfaces of the plate. Prescribed temperature at the top and bottom surfaces are the thermal boundary conditions usually were considered in the literature for FG beams and plates analyses. Hence, for brevity purpose and without loss of generality, here these types of the boundary conditions are considered, which for plate problem become

$$T = T_m \text{ at } z = -\frac{h}{2} \text{ and } T = T_c \text{ at } z = \frac{h}{2} \quad (4a,b)$$

For the case of power law distribution, the solution of Eq. (3) subjected to the boundary conditions (4a,b) can be obtained by means of polynomial series solutions Lanhe (2004). The result is

$$T(z) = T_m + \frac{\Delta T}{C} \left[ \left( \frac{2z+h}{2h} \right) - \frac{K_{cm}}{(p+1)K_m} \left( \frac{2z+h}{2h} \right)^{p+1} + \frac{K_{cm}^2}{(2p+1)K_m^2} \left( \frac{2z+h}{2h} \right)^{2p+1} - \frac{K_{cm}^3}{(3p+1)K_m^3} \left( \frac{2z+h}{2h} \right)^{3p+1} + \frac{K_{cm}^4}{(4p+1)K_m^4} \left( \frac{2z+h}{2h} \right)^{4p+1} - \frac{K_{cm}^5}{(5p+1)K_m^5} \left( \frac{2z+h}{2h} \right)^{5p+1} \right] \quad (5)$$

where  $K_{cm} = K_c - K_m$  and

$$C = 1 - \frac{K_{cm}}{(p+1)K_m} + \frac{K_{cm}^2}{(2p+1)K_m^2} - \frac{K_{cm}^3}{(3p+1)K_m^3} + \frac{K_{cm}^4}{(4p+1)K_m^4} - \frac{K_{cm}^5}{(5p+1)K_m^5}$$

Table 1 Temperature-dependent coefficients of material properties for ceramic ( $ZrO_2$ ) and metals (Ti-6Al-4V) (Ref. [17]).

	Material	$G_{-1}$	$G_0$	$G_1$	$G_2$	$G_3$
$E$	Ti-6Al-4V	0	122.7	$-4.605 \times 10^{-4}$	0	0
	ZrO <sub>2</sub>	0	132.2	$-3.805 \times 10^{-4}$	$-6.127 \times 10^{-8}$	0
$\nu$	Ti-6Al-4V	0	0.2888	$-1.108 \times 10^{-4}$	0	0
	ZrO <sub>2</sub>	0	0.3330	0	0	0
$\alpha$	Ti-6Al-4V	0	$7.43 \times 10^{-6}$	$7.483 \times 10^{-4}$	$-3.621 \times 10^{-7}$	0
	ZrO <sub>2</sub>	0	$13.3 \times 10^{-6}$	$-1.421 \times 10^{-3}$	$9.549 \times 10^{-7}$	0
$K$	Ti-6Al-4V	0	6.10	0	0	0
	ZrO <sub>2</sub>	0	1.78	0	0	0

Due to axisymmetric temperature distribution and the geometrical periodicity of the annular plate, the displacement components of an arbitrary point within the plate are assumed to be  $u_0 = u_0(r, z)$  and  $w_0 = w_0(r, z)$ , i.e. the displacements of an arbitrary point of plate along the  $r$ - and  $z$ -directions, respectively. Hereafter, a subscript '0' is used to represent the deformation field variables and the stress components in the initial equilibrium state of the plate under thermal loading.

The thermoelastic equilibrium equations and the related boundary conditions can be obtained by using the virtual work principle

$$\int_{-\frac{h}{2}}^{\frac{h}{2}} \int_0^{2\pi} \int_{R_i}^{R_o} (\sigma_{0rr} \delta \varepsilon_{0rr} + \sigma_{0\theta\theta} \delta \varepsilon_{0\theta\theta} + \sigma_{0zz} \delta \varepsilon_{0zz} + \sigma_{0rz} \delta \gamma_{0rz}) r dr d\theta dz \tag{6}$$

where  $\varepsilon_{0ii}$  and  $\sigma_{0ii}$  ( $i = r, \theta, z$ ) are the normal components of the strain and stress tensor, respectively;  $\gamma_{0rz}$  and  $\sigma_{0rz}$  are the shear components of the strain and the stress tensor. Also, the integral in this equation represent the variation of the elastic potential energy of the plate.

Employing the small deformation assumption, the strain-displacement relations become

$$\varepsilon_{0rr} = \frac{\partial u_0}{\partial r}, \varepsilon_{0\theta\theta} = \frac{u_0}{r}, \varepsilon_{0zz} = \frac{\partial w_0}{\partial z}, \gamma_{0rz} = \frac{\partial u_0}{\partial z} + \frac{\partial w_0}{\partial r} \tag{7a-d}$$

Also, the stress-strain relations can be written as

$$\begin{Bmatrix} \sigma_{0rr} \\ \sigma_{0\theta\theta} \\ \sigma_{0zz} \\ \sigma_{0rz} \end{Bmatrix} = \begin{bmatrix} C_{11} & C_{12} & C_{13} & 0 \\ C_{12} & C_{22} & C_{23} & 0 \\ C_{13} & C_{23} & C_{33} & 0 \\ 0 & 0 & 0 & C_{55} \end{bmatrix} \begin{Bmatrix} \varepsilon_{0rr} - \alpha \Delta T \\ \varepsilon_{0\theta\theta} - \alpha \Delta T \\ \varepsilon_{0zz} - \alpha \Delta T \\ \gamma_{0rz} \end{Bmatrix} \tag{8}$$

where  $C_{pq} = [C_{pq}(z, T); p, q = 1, 2, 3]$  are the elastic constants;  $\alpha = [\alpha(z, T)]$  is the thermal expansion coefficient and  $\Delta T = [T(z) - T_0]$  is the temperature rise at an arbitrary material point of the plate. The material elastic coefficients  $C_{pq}$  for an isotropic plate are related to the elastic material properties as follows

$$C_{11} = C_{22} = C_{33} = \frac{(1 - \nu)E}{(1 + \nu)(1 - 2\nu)}, C_{12} = C_{23} = C_{33} = \frac{\nu E}{(1 + \nu)(1 - 2\nu)}, C_{55} = \frac{E}{2(1 + \nu)} \tag{9a-c}$$

where  $E = [E(z, T)]$  and  $\nu = [\nu(z, T)]$  are Young's modulus and Poisson's ratio, respectively.

Substituting Eqs. (7) and (8) into Eq. (6) and performing the integration by part, the thermoelastic equilibrium equations and the related boundary conditions can be derived in terms of the displacement components as,

*Thermoelastic equilibrium equations*

$$\delta u_0 ; C_{11} \frac{\partial^2 u_0}{\partial r^2} + C_{12} \frac{\partial u_0}{r \partial r} - C_{12} \frac{u_0}{r^2} + C_{13} \frac{\partial^2 w_0}{\partial r \partial z} + C'_{55} \frac{\partial u_0}{\partial z} + C'_{55} \frac{\partial w_0}{\partial r} + C_{55} \frac{\partial^2 u_0}{\partial z^2} +$$

$$\begin{aligned}
& C_{55} \frac{\partial^2 w_0}{\partial r \partial z} + \left( \frac{C_{11} - C_{12}}{r} \right) \frac{\partial u_0}{\partial r} + \left( \frac{C_{12} - C_{22}}{r} \right) \frac{u_0}{r} + \left( \frac{C_{13} - C_{23}}{r} \right) \frac{\partial w_0}{\partial z} \\
& = \frac{1}{r} (C_{11} + C_{13} - C_{22} - C_{23}) \alpha \Delta T
\end{aligned} \tag{10}$$

$$\begin{aligned}
& \delta w_0 ; (C_{55} + C_{13}) \frac{\partial^2 u_0}{\partial r \partial z} + C_{55} \frac{\partial^2 w_0}{\partial r^2} + C'_{13} \frac{\partial u_0}{\partial r} + \frac{C'_{23}}{r} u_0 + \left( \frac{C_{23} + C_{55}}{r} \right) \frac{\partial u_0}{\partial z} + C'_{33} \frac{\partial w_0}{\partial z} + \\
& C_{33} \frac{\partial^2 w_0}{\partial z^2} + \frac{C_{55}}{r} \frac{\partial w_0}{\partial r} = (C'_{13} + C'_{23} + C'_{23}) \alpha \Delta T + (C_{13} + C_{23} + C_{33}) (\alpha \Delta T)'
\end{aligned} \tag{11}$$

Boundary conditions at the edges  $r = R_i$  and  $r = R_o$

$$\text{Either } \delta u_0 = 0 \text{ or } C_{11} \frac{\partial u_0}{\partial r} + \frac{C_{12}}{r} u_0 + C_{13} \frac{\partial w_0}{\partial z} - (C_{11} + C_{12} + C_{13}) \alpha \Delta T = 0 \tag{12a,b}$$

$$\text{Either } \delta w_0 = 0 \text{ or } C_{55} \frac{\partial u_0}{\partial z} + C_{55} \frac{\partial w_0}{\partial r} = 0 \tag{13a,b}$$

Boundary conditions at the surface ( $z = -h/2$ )

$$\text{Either } \delta u_0 = 0 \text{ or } C_{55} \frac{\partial u_0}{\partial z} + C_{55} \frac{\partial w_0}{\partial r} = 0 \tag{14a,b}$$

$$\text{Either } \delta w_0 = 0 \text{ or } C_{13} \frac{\partial u_0}{\partial r} + \frac{C_{23}}{r} u_0 + C_{33} \frac{\partial w_0}{\partial z} - (C_{13} + C_{23} + C_{33}) \alpha \Delta T = 0 \tag{15a,b}$$

Boundary conditions at the surface ( $z = h/2$ )

$$\text{Either } \delta u_0 = 0 \text{ or } C_{55} \frac{\partial u_0}{\partial r} + C_{55} \frac{\partial w_0}{\partial r} = 0 \tag{16a,b}$$

$$\text{Either } \delta w_0 = 0 \text{ or } C_{13} \frac{\partial u_0}{\partial r} + \frac{C_{23}}{r} u_0 + C_{33} \frac{\partial w_0}{\partial z} - (C_{13} + C_{23} + C_{33}) \alpha \Delta T = 0 \tag{17a,b}$$

where  $(\bullet)' = \frac{d}{dz}(\bullet)$ .

### 2.3. Equilibrium under thermo-mechanical loading

Under the action of axisymmetric mechanical loading, the total displacement components measured

from the plate undeformed configurations become  $u_0(r, z) + u(r, z)$  and  $w_0(r, z) + w(r, z)$  along the  $r$ - and  $z$ -directions, respectively. The equilibrium equations with the related boundary conditions can be obtained using the virtual work principle

$$\int_{-h/2}^h \int_{R_i}^{R_o} \int_0^{2\pi} [(\sigma_{rr} + \sigma_{0rr})\delta\varepsilon_{rr} + (\sigma_{\theta\theta} + \sigma_{0\theta\theta})\delta\varepsilon_{\theta\theta} + (\sigma_{rz} + \sigma_{0rz})\delta\gamma_{rz}] r d\theta dr dz - \int_{R_i}^{R_o} \int_0^{2\pi} q \delta w|_{z=h/2} r d\theta dr = 0 \quad (18)$$

where the first integral represent the virtual work of the internal forces including the initial thermal stresses and the second integral is the virtual work of the external load  $q(r)$  acting on the top surface of the plate. Note that  $(\varepsilon_{ii}, \gamma_{rz})$  and  $(\sigma_{ib}, \sigma_{rz})$  with  $i = r, \theta, z$  are the strain and the stress tensor components due to external mechanical loading, respectively. Also, since, the displacement components at equilibrium state are known, one has  $\delta\varepsilon_{0rr} = \delta\varepsilon_{0\theta\theta} = \delta\varepsilon_{0zz} = \delta\gamma_{0rz} = 0$  and hence they are not included in Eq. (18).

By considering the constitutive relations for the mechanical stress-strain, the thermal equilibrium equations (10) and (11) and performing the integration by parts from Eq. (18) with respect to spatial coordinate variables  $r$  and  $z$ , the equilibrium equations and the related boundary conditions can be obtained as follows

$$\delta u ; (\sigma_{0rr} + C_{11}) \frac{\partial^2 u}{\partial r^2} + \frac{(C_{11} + \sigma_{0\theta\theta})}{r} \frac{\partial u}{\partial r} + (C_{55} + \sigma_{0zz}) \frac{\partial^2 u}{\partial z^2} + C'_{55} \frac{\partial u}{\partial z} + 2\sigma_{0rz} \frac{\partial^2 u}{\partial r \partial z} - \frac{(\sigma_{0\theta\theta} + C_{22})}{r^2} u + (C_{55} + C_{13}) \frac{\partial^2 w}{\partial r \partial z} + C'_{55} \frac{\partial w}{\partial r} + \left( \frac{C_{13} - C_{23}}{r} \right) \frac{\partial w}{\partial z} = 0 \quad (19)$$

$$\delta w ; (\sigma_{0rr} + C_{55}) \frac{\partial^2 w}{\partial r^2} + \frac{(\sigma_{0\theta\theta} + C_{55})}{r} \frac{\partial w}{\partial r} + (\sigma_{0zz} + C_{33}) \frac{\partial^2 w}{\partial z^2} + C'_{33} \frac{\partial w}{\partial z} + 2\sigma_{0rz} \frac{\partial^2 w}{\partial r \partial z} + (C_{13} + C_{55}) \frac{\partial^2 u}{\partial z \partial r} + \left( \frac{C_{23} + C_{55}}{r} \right) \frac{\partial u}{\partial z} + \frac{C'_{23}}{r} u + C'_{13} \frac{\partial u}{\partial r} = 0 \quad (20)$$

*Boundary conditions at the surfaces  $r = R_i$  and  $r = R_o$*

$$\text{Either } \delta u = 0 \text{ or } (C_{11} + \sigma_{0rr}) \left( \frac{\partial u}{\partial r} \right) + \sigma_{0rz} \left( \frac{\partial u}{\partial z} \right) + \frac{C_{12}}{r} u + C_{13} \frac{\partial w}{\partial z} = 0 \quad (21a,b)$$

$$\text{Either } \delta w = 0 \text{ or } (C_{55} + \sigma_{0rr}) \left( \frac{\partial w}{\partial r} \right) + \sigma_{0rz} \left( \frac{\partial w}{\partial z} \right) + C_{55} \frac{\partial u}{\partial z} = 0 \quad (22a,b)$$

*Boundary conditions at the surface ( $z = -h/2$ )*

$$\text{Either } \delta u = 0 \text{ or } \sigma_{0rz} \left( \frac{\partial u}{\partial r} \right) + (\sigma_{0zz} + C_{55}) \left( \frac{\partial u}{\partial z} \right) + C_{55} \frac{\partial w}{\partial r} = 0 \quad (23a,b)$$

$$\text{Either } \delta w = 0 \text{ or } C_{13} \frac{\partial u}{\partial r} + \frac{C_{23}}{r} u + \sigma_{0rz} \left( \frac{\partial w}{\partial r} \right) + (\sigma_{0zz} + C_{33}) \left( \frac{\partial w}{\partial z} \right) = 0 \quad (24a,b)$$

Boundary conditions at the surface ( $z = h/2$ )

$$\text{Either } \delta u = 0 \text{ or } \sigma_{0rz} \left( \frac{\partial u}{\partial r} \right) + (\sigma_{0zz} + C_{55}) \left( \frac{\partial u}{\partial z} \right) + C_{55} \frac{\partial w}{\partial r} = 0 \quad (25a,b)$$

$$\text{Either } \delta w = 0 \text{ or } C_{13} \frac{\partial u}{\partial r} + \frac{C_{23}}{r} u + \sigma_{0rz} \left( \frac{\partial w}{\partial r} \right) + (\sigma_{0zz} + C_{33}) \left( \frac{\partial w}{\partial z} \right) = -q(r) \quad (26a,b)$$

### 3. Solution procedure

If it is not impossible to solve the above system of equations analytically, it is very difficult to obtain such a solution. Therefore, here the differential quadrature method as an efficient and accurate numerical tool (Malekzadeh 2009, Malekzadeh *et al.* 2010a, Bert and Malik 1996, Malekzadeh *et al.* 2010b, Malekzadeh *et al.* 2008) is employed to solve these systems of equations.

The basic idea of the differential quadrature method is that the derivative of a function, with respect to a coordinate variable at a given sampling point, is approximated as the linear weighted sums of its values at all of the sampling points in the domain of that variable. In order to illustrate the DQ approximation, consider a function  $f(\xi, \eta)$  having its field on a domain  $a_\xi \leq \xi \leq b_\xi$  and  $a_\eta \leq \eta \leq b_\eta$ . Let, in the given domain, the function values be known or desired on a grid of sampling point. According to the DQ method, the derivatives of a function  $f(\xi, \eta)$  can be approximated as

$$\begin{aligned} \left. \frac{\partial f(\xi, \eta)}{\partial \xi} \right|_{(\xi_p, \eta_j)} &= \sum_{k=1}^{N_\xi} A_{ik}^\xi f(\xi_k, \eta_j) = \sum_{k=1}^{N_\xi} A_{ik}^\xi f_{kj}, \quad \left. \frac{\partial^2 f(\xi, \eta)}{\partial \xi^2} \right|_{(\xi_p, \eta_j)} = \sum_{k=1}^{N_\xi} B_{ik}^\xi f_{kj} \\ \left. \frac{\partial f(\xi, \eta)}{\partial \eta} \right|_{(\xi_p, \eta_j)} &= \sum_{k=1}^{N_\eta} A_{jk}^\eta f_{ik}, \quad \left. \frac{\partial^2 f(\xi, \eta)}{\partial \eta^2} \right|_{(\xi_p, \eta_j)} = \sum_{k=1}^{N_\eta} B_{jk}^\eta f_{ik}, \\ \left. \frac{\partial^2 f(\xi, \eta)}{\partial \xi \partial \eta} \right|_{(\xi_p, \eta_j)} &= \sum_{l=1}^{N_\eta} \sum_{k=1}^{N_\xi} A_{ik}^\xi A_{jl}^\eta f_{kl} \quad \text{for } i = 1, 2, \dots, N_\xi \end{aligned} \quad (27a-e)$$

From this equation one can deduce that the important components of DQ approximations are weighting coefficients and the choice of sampling points. In order to determine the weighting coefficients a set of test functions should be used in Eq. (27). For polynomial basis functions DQ, a set of Lagrange polynomials are employed as the test functions. The weighting coefficients for the first-order derivatives in the  $\xi$ -direction are thus determined as (Bert and Malik 1996)

$$A_{ij}^\xi = \begin{cases} \frac{1}{(b_\xi - a_\xi)(\xi_i - \xi_j)} \frac{M(\xi_i)}{M(\xi_j)} & \text{for } i \neq j \\ -\sum_{\substack{j=1 \\ j \neq i}}^{N_\xi} A_{ij}^\xi & \text{for } i = j \end{cases}; i, j = 1, 2, \dots, N_\xi \quad (28)$$

where  $M(\xi_i) = \prod_{K=1, j \neq k}^{N_\xi} (\xi_i - \xi_k)$ .

The weighting coefficients of the second order derivative can be obtained as (Bert and Malik 1996)

$$[B_{ij}^\xi] = [A_{ij}^\xi][A_{ij}^\xi] = [A_{ij}^{\xi^2}] \tag{29}$$

In a similar manner the weighting coefficients along the  $\eta$ -direction can be obtained. In the numerical computations, the roots of Chebyshev polynomials are used (Bert and Malik 1996)

$$\mu_i = a_\mu + \frac{(b_\mu - a_\mu)}{2} \left\{ 1 - \cos \left[ \frac{(i-1)\pi}{(N_\mu - 1)} \right] \right\} \text{ for } i = 1, 2, \dots, N_\mu \text{ and } \mu = \xi, \eta \tag{30}$$

In employing the DQ method, the equilibrium equations are discretized at the domain grid points  $(r_i, z_j)$  with  $i = 2, 3, \dots, N_r - 1$  and  $j = 2, 3, \dots, N_z - 1$ . And the boundary conditions are discretized at the boundary grid points  $(r_i, z_j)$  with  $i = 1, N_r$  and  $j = 1, N_z$ . Here,  $r_1 = R_i, r_{N_r} = R_0$  and  $z_1 = -h / 2, z_{N_z} = h / 2$ .

In this study, without loss of generality, the number of DQ grid points in the thickness and the radial directions are assumed to be equal and they are taken to be  $N_r = N_z = N$ . Here for brevity purpose, only the DQ discretized forms of the thermal equilibrium equations are presented and the other equations can be discretized in a similar manner.

Eq. (10)

$$\begin{aligned} & (C_{11})_j \sum_{k=1}^{N_r} B_{ik}^r u_{0kj} + \frac{(C_{12})_j}{r_i} \sum_{k=1}^{N_r} A_{ik}^r u_{0kj} - \frac{(C_{12})_j}{r_i^2} u_{0ij} + (C_{13})_j \sum_{k=1}^{N_r} \sum_{l=1}^{N_z} A_{ik}^r A_{jl}^z w_{0kl} + \\ & (C'_{55})_j \sum_{l=1}^{N_z} A_{jk}^z u_{0ik} + (C'_{55})_j \sum_{k=1}^{N_r} A_{ik}^r w_{0kj} + (C_{55})_j \sum_{k=1}^{N_r} \sum_{l=1}^{N_z} A_{ik}^r A_{jl}^z w_{0kl} + (C_{55})_j \sum_{l=1}^{N_z} B_{jk}^z u_{0kl} + \\ & \frac{(C_{11} - C_{12})}{r_i} \sum_{k=1}^{N_r} A_{ik}^r u_{0kj} + \frac{(C_{12} - C_{22})}{r_i^2} u_{0ij} + \frac{(C_{13} - C_{23})_j}{r_i} \sum_{l=1}^{N_z} A_{jk}^z w_{0il} = \\ & \frac{[(C_{11} + C_{13} - C_{22} - C_{23}) \alpha \Delta T]_j}{r_i} \end{aligned} \tag{31}$$

Eq. (11)

$$\begin{aligned} & (C_{55} + C_{13})_j \sum_{k=1}^{N_r} \sum_{l=1}^{N_z} A_{ik}^r A_{jl}^z u_{0kl} + (C_{55})_j \sum_{k=1}^{N_r} B_{ik}^r w_{0kj} + (C'_{13})_j \sum_{k=1}^{N_r} A_{ik}^r u_{0kj} + \frac{(C'_{23})_j}{r_i} u_{0ij} + \\ & \frac{(C_{23} + C_{55})_j}{r_i} \sum_{l=1}^{N_z} A_{jk}^z u_{0il} + (C'_{33})_j \sum_{l=1}^{N_z} A_{jk}^z w_{0il} + (C_{33})_j \sum_{l=1}^{N_z} B_{jk}^z w_{0il} + \frac{(C_{55})_j}{r_i} \sum_{k=1}^{N_r} A_{ik}^r w_{0kj} \\ & = (C'_{13} + C'_{23} + C'_{33})_j (\alpha \Delta T)_j + (C_{13} + C_{23} + C_{33})_j (\alpha \Delta T)_j \end{aligned} \tag{32}$$

where  $i = 2, 3, \dots, N_r - 1$ , and  $i = 2, 3, \dots, N_z - 1$ , After discretizing the governing equations, one obtains a system of linear algebraic equations which in the matrix form become

$$[SK_o][U_0] = \{f_0\} \quad (33)$$

Where  $\{U_0\} = [\{u_0\} \{W_0\}]^T$  is the matrix of unknown degrees of freedom of all layers,  $[SK_o]$  and  $\{f_0\}$  are the stiffness matrix and the load vector, respectively.

After solving these equations, the initial thermal stresses at each DQ grid points are obtained from the constitutive relations (8) as

$$\left\{ \begin{array}{l} (\sigma_{0rr})_{ij} \\ (\sigma_{0\theta\theta})_{ij} \\ (\sigma_{0zz})_{ij} \\ (\sigma_{0rz})_{ij} \end{array} \right\} = \left[ \begin{array}{cccc} (C_{11})_j & (C_{12})_j & (C_{13})_j & 0 \\ (C_{12})_j & (C_{22})_j & (C_{23})_j & 0 \\ (C_{13})_j & (C_{23})_j & (C_{33})_j & 0 \\ 0 & 0 & 0 & (C_{55})_j \end{array} \right] \left\{ \begin{array}{l} \sum_{k=1}^{N_r} A_{ik}^r u_{0kj} - (\alpha\Delta T)_j \\ \frac{u_{0ij}}{r_i} - (\alpha\Delta T)_j \\ \sum_{l=1}^{N_z} A_{jk}^z w_{0lk} - (\alpha\Delta T)_j \\ \sum_{l=1}^{N_z} A_{ik}^z u_{0lk} + \sum_{k=1}^{N_r} A_{ik}^r w_{0kj} \end{array} \right\} \quad (34)$$

In a similar manner as those of the thermoelastic equilibrium equations, the DQ rules can be employed to discretize the thermo-mechanical governing equations. Then, by solving the resulting system of algebraic equations, the displacement and stress components are obtained.

#### 4. Numerical results

In this section, firstly, the fast rate of convergence and the accuracy of the method are investigated. Then, the effects of the different geometrical parameters, the uniform and non-uniform temperature rise and the temperature-dependence of material properties on the thermo-mechanical bending response of FG circular and annular plates are presented.

In the numerical calculation, the following dimensionless quantities are introduced

$$-\frac{1}{2} \leq \eta (=z/h) \leq \frac{1}{2}, 0 < \xi \left( = \frac{r - R_i}{R_o - R_i} \right) \leq 1, \lambda = \frac{R_i}{R_o}, U = \frac{u E_{0c}}{q_0 R_o}, W = \frac{w E_{0c}}{q_0 R_o},$$

$$\sum_{rz} = \frac{\sigma_{0rz} + \sigma_{rz}}{q_0}, \sum_{ii} = \frac{\sigma_{0ii} + \sigma_{ii}}{q_0}, (i=r, \theta, z) \quad (35a-g)$$

where  $q_0$  is the intensity of the mechanical loading, which is assumed to be uniform and exists in all solved examples. Also, in all numerical computation a value of  $R_0 = 1$  m is used.

The material properties of Ti-6Al-4V and ZrO<sub>2</sub>, as given in Table 1, are used in the numerical computations, which are chosen from the work of Kim (2005). They are valid for the temperature range of

300 K ≤ T ≤ 1100K. Also, the stress free temperature is assumed to have the value of T<sub>0</sub> = 300 K. Otherwise specified, the plate is subjected to non-uniform temperature rise and ΔT = 800 K.

As a first example, the convergence behavior for the displacement components and the radial normal and transverse shear stress components of the FG annular plates are presented in Tables 2 and 3, respectively. Fast rate of convergence of the method for both displacement and stress components is quite obvious. Also, one can see that in all cases under consideration, 21 and 27 DQ grid points are sufficient to obtain the displacement and stress components, respectively.

To validate the presented formulations and the method of solution, results for FG circular plates with clamped edge are compared with those obtained by Reddy *et al.* (1999) and Li *et al.* (2008) based on the FSDT in Table 4. Also for the case of rolled simply supported FG circular plates, results of the present approach are compared with those of Reddy *et al.* (1999) in Table 5 for different values of the material grad index (p) and the thickness-to-outer radius ratio of plate. It should be mentioned that the material properties and other parameters are the same to those used by Reddy *et al.* (1999). In all cases, good agreement between the results of the present approach and the other methods exist.

After demonstrating the fast rate of convergence and accuracy of the method, at this stage the effects of different parameters on the bending response of the annular plates are investigated.

As a first example, the effects of the uniform and the non-uniform temperature rise on the deflection and stress components of the FG annular plates with both edges clamped are shown in Figs. 2 and 3, respectively. In Fig. 2(a) and 2(b), the variation of the deflection at the central point of the plate (ξ = 0.5, η = 0) verses the uniform and non-uniform temperature rise and its variation along the radial

Table 2 Convergence of the non-dimensional displacement components of the clamped-clamped FG annular plate [λ = 0.5, p = 1, ΔT = 800K]\*

N	Uniform temperature rise				Non-Uniform temperature rise			
	h / R <sub>o</sub> = 0.2		h / R <sub>o</sub> = 0.5		h / R <sub>o</sub> = 0.2		h / R <sub>o</sub> = 0.5	
	U	W	U	W	U	W	U	W
11	-0.0644	-1.5086	-0.0209	-0.3958	-0.0463	-1.0131	-0.0148	-0.2688
15	-0.0634	-1.5140	-0.0205	-0.3939	-0.0456	-1.0149	-0.0145	-0.2672
19	-0.0632	-1.5160	-0.0203	-0.3936	-0.0455	-1.0161	-0.0144	-0.2671
21	-0.0632	-1.5165	-0.0203	-0.3935	-0.0455	-1.0164	-0.0143	-0.2670
25	-0.0632	-1.5166	-0.0203	-0.3935	-0.0455	-1.0164	-0.0143	-0.2670

\*U = U(0.5, 0.5), W = W(0.5,0)

Table 3 Convergence of the non-dimensional stress components of the clamped-clamped FG annular plate [λ = 0.5, p = 1, ΔT = 800K]\*

N	Uniform temperature rise				Non-Uniform temperature rise			
	h / R <sub>o</sub> = 0.2		h / R <sub>o</sub> = 0.5		h / R <sub>o</sub> = 0.2		h / R <sub>o</sub> = 0.5	
	Σ <sub>rr</sub>	Σ <sub>rz</sub>	Σ <sub>rr</sub>	Σ <sub>rz</sub>	Σ <sub>rr</sub>	Σ <sub>rz</sub>	Σ <sub>rr</sub>	Σ <sub>rz</sub>
15	-2.4213	0.0568	-1.1743	0.0375	-1.8807	0.0532	-0.9925	0.0369
19	-2.4092	0.0567	-1.1341	0.0374	-1.8686	0.0531	-0.9586	0.0368
23	-2.4050	0.0566	-1.1145	0.0373	-1.8642	0.0531	-0.9419	0.0367
27	-2.4036	0.0565	-1.1037	0.0373	-1.8625	0.0531	-0.9326	0.0367
29	-2.4036	0.0565	-1.1037	0.0373	-1.8624	0.0531	-0.9266	0.0367

\*Σ<sub>rr</sub> = Σ<sub>rr</sub>(0.5, 0.5), Σ<sub>rz</sub> = Σ<sub>rz</sub>(0.5,0).

Table 4 Comparison of the non-dimensional deflection of the uniformly loaded FG clamped circular plate ( $\nu = 0.288 E_m / E_c = 0.396$ )

$h / R_o$	Theory	Material graded index ( $p$ )						
		0	2	4	10	25	50	100
0.05	Present	2.548	1.399	1.279	1.152	1.075	1.044	1.027
	FSDT [4]	2.554	1.402	1.282	1.155	1.077	1.046	1.029
	Elasticity [9]	2.561	1.405	1.282	1.157	-	1.049	1.032
0.1	Present	2.629	1.438	1.313	1.185	1.107	1.076	1.059
	FSDT [4]	2.639	1.444	1.320	1.190	1.112	1.080	1.063
	Elasticity [9]	2.667	1.456	1.329	1.201	-	1.091	1.074
0.2	Present	2.957	1.597	1.456	1.319	1.239	1.207	1.190
	FSDT [4]	2.979	1.613	1.473	1.333	1.250	1.216	1.199
	Elasticity [9]	3.093	1.658	1.511	1.375	-	1.262	1.244

Table 5 Comparison of the non-dimensional deflection of uniformly loaded FG rolled simply supported circular plate ( $\nu = 0.288 E_m / E_c = 0.396$ )

$p$	Thickness to radius ratio ( $h / R_o$ )							
	0.05		0.1		0.15		0.2	
	present	FSDT [4]	present	FSDT [4]	present	FSDT [4]	present	FSDT [4]
0	10.382	10.396	10.456	10.481	10.576	10.623	10.735	10.822
4	5.216	5.223	5.249	5.261	5.301	5.325	5.374	5.414
10	4.697	4.704	4.728	4.739	4.776	4.799	4.843	4.882
25	4.381	4.386	4.411	4.421	4.458	4.478	4.523	4.559
50	4.253	4.258	4.287	4.258	4.329	4.349	4.394	4.429
10 <sup>2</sup>	4.185	4.189	4.214	4.189	4.261	4.280	4.325	4.359

direction for a given temperature rise is shown, respectively. It can be seen from Fig. 2(a) and 2(b) that for the same value of temperature rise, the uniform temperature rise has more effect than the non-uniform temperature rise on the results and by increasing the temperature rise, the discrepancy between the results increase dramatically. This may be due to the fact that for uniform temperature rise the material properties of the whole plate decrease in spite of the non-uniform temperature rise that changes only those of some part of the plate. Hence, in the uniform case, the stiffness of plate decreases more than the non-uniform case. The same behavior was observed for the natural frequencies of the FG beams and plates (Malekzadeh *et al.* 2010a, Bert and Malik 1996, Malekzadeh *et al.* 2010b). In Fig. 2(c) and 2(d), the variation of the in-plane displacement component along the thickness direction and the radial direction are presented ( $\Delta T = 800$  K). It can be seen that uniform temperature rise increases its value at a given section but the non-uniform temperature rise considerably affects its behavior along the radial direction. In Fig. 3, the variation of the stress components across the plate thickness (at  $\xi = 0.5$ ) verses the uniform and non-uniform temperature rise are shown. It should be mentioned that  $\Sigma_{\theta\theta}$  has a similar behavior as  $\Sigma_{rr}$  and hence it is not presented here for brevity. It is observed that non-uniform temperature affects the radial and normal components of the stress and uniform temperature rise change the transverse shear stress. Also, the most discrepancy between the results for  $\Sigma_{rr}$  occurs at the top surface (ceramic rich) of the plate.

The effect of temperature-dependence of the material properties on the bending response of FG plate is

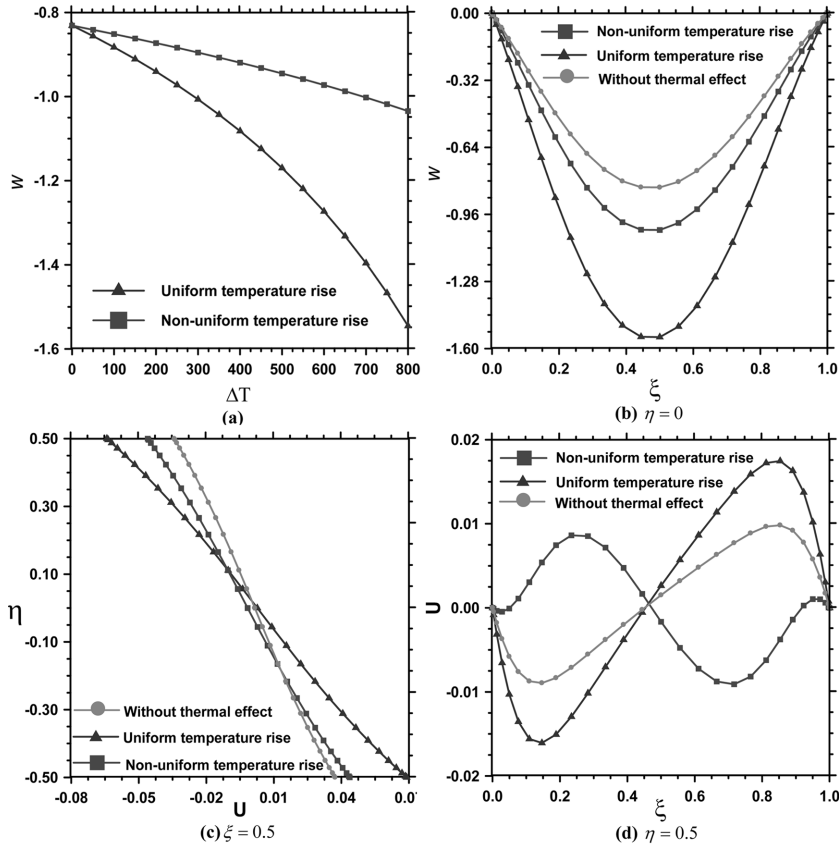


Fig. 2 (a)-(d). Effect of uniform and non-uniform temperature rise on the non-dimensional displacement components of the clamped-clamped FG annular plate ( $\lambda = 0.5$ ,  $h / R_o = 0.2$ ,  $p = 2$ ).

shown by studying the variation of the displacement and the stress components of the FG clamped-clamped annular plates subjected to non-uniform temperature rise. In Figs. 4 and 5, the results for the displacement and the stress components are presented, respectively. It is obvious that the displacements are greatly underestimated when the temperature-dependence of the material parameters is not taken into account. The discrepancy between the temperature-dependent and temperature independent solution for the deflection increases dramatically as the temperature rise increases. The effect of temperature-dependence of material can also be seen on the stress components especially on the radial and shear stress component.

In some previous analysis of FG plates in thermal environment, the pre-stress analysis was not performed and the initial thermal stresses were usually obtained approximately from the thermal strains; see for example (Kim 2005 and Prakash and Garapathi 2006). For the circular plates under axisymmetric thermal loading, based on elasticity theory these approximate formulations reduce to

$$\begin{aligned} \sigma_{0rr} &= -(C_{11} + C_{12} + C_{13}) \alpha(z, T) \Delta T, & \sigma_{0\theta\theta} &= -(C_{12} + C_{22} + C_{23}) \alpha(z, T) \Delta T \\ \sigma_{0zz} &= -(C_{13} + C_{23} + C_{33}) \alpha(z, T) \Delta T, & \sigma_{0rz} &= 0 \end{aligned} \quad (36)$$

Here, comparisons between the results obtained for FG annular plate based on the exact analysis presented in Sec. 2.2 and the approximate formulation (36) for the initial thermal stresses, are presented. In Table

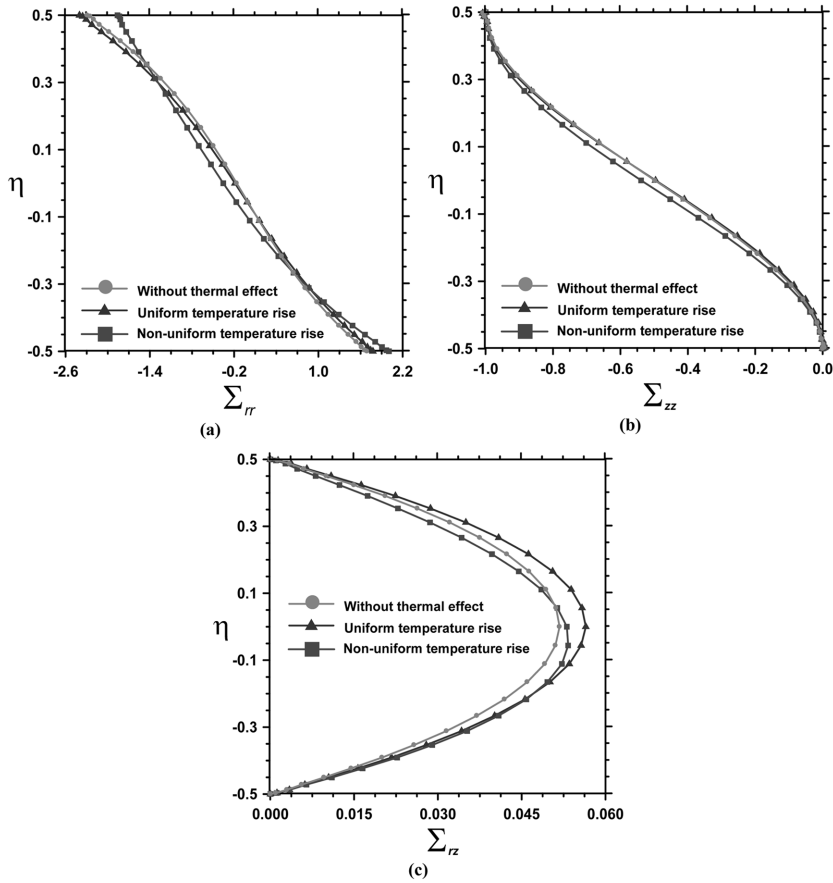


Fig. 3 (a)-(c). Variation of the non-dimensional stress components across the thickness of the clamped-clamped FG annular plate with uniform and non-uniform temperature rise ( $\lambda = 0.5, p = 2, \xi = 0.5, h/R_o = 0.2$ ).

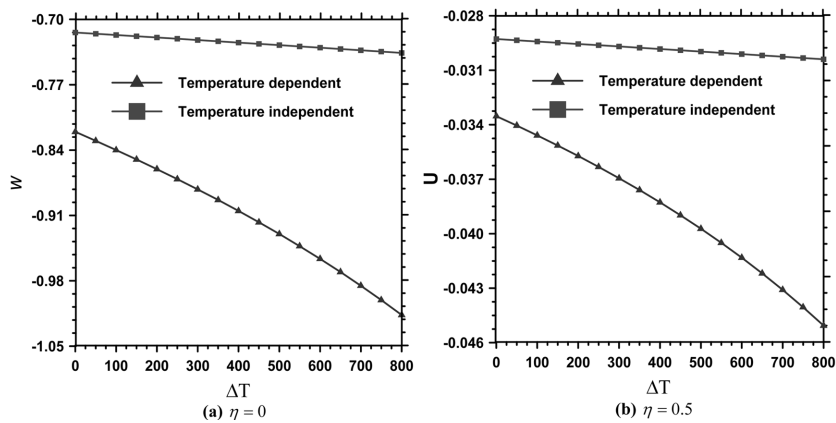


Fig. 4 (a)-(c). Effect of the temperature-dependence of the material properties on the non-dimensional displacement components of the clamped-clamped FG annular plate ( $\lambda = 0.5, p = 1, \xi = 0.5, h/R_o = 0.2$ ).

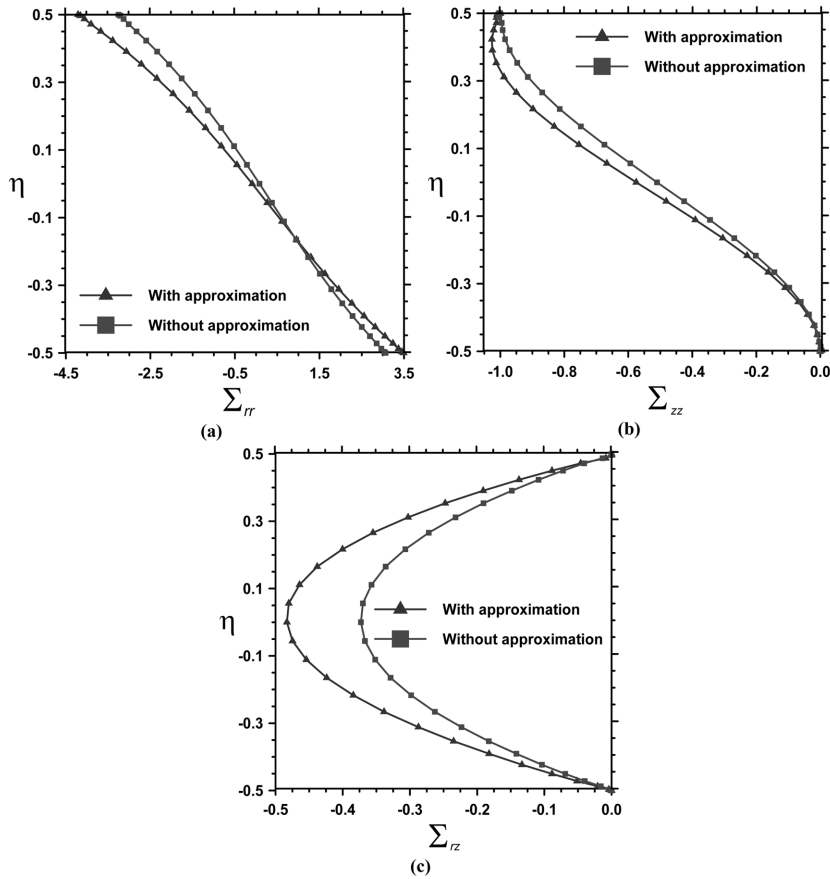


Fig. 5 (a)-(c). Effect of the temperature-dependence of the material properties on the non-dimensional stress component of the clamped-clamped FG annular plate ( $\lambda = 0.5$ ,  $\xi = 0.5$ ,  $p = 1$ ,  $h/R_o = 0.2$ ).

6, the percentages of the difference between the results of the two approaches for the deflection and the transverse shear stress and for two different sets of boundary conditions are given. It is interesting to note that the difference between the two approaches is 14.94% and 22.8% for the deflection and the transverse shear stress component of the clamped-simply supported FG annular plate, respectively. Also, the difference between the results of the two approaches increases as the temperature rise increases.

In Fig. 6, the components of stress tensor obtained based on the two approaches are compared. Based on the results presented in Table 6 and Fig. 6, one can see that the exact evaluation of initial thermal stress is essential for an accurate bending analysis of FG plates.

The effect of geometrical parameters on the response of the FG annular plates for two different set of boundary conditions are presented in Table 7. It can be seen that increasing the inner-to-outer radius ratio and thickness-to-outer radius ratio causes the center deflection to decrease monotonically.

## 5. Conclusions

The axisymmetric bending analysis of FG annular plates with temperature-dependent material

Table 6 The percent of the difference between the results for the deflection and the transverse shear stress for the FG annular plate with and without approximation subjected to non-uniform temperature rise ( $\xi = 0.5, \eta = 0$ )

Boundary conditions		$\Delta T(K)$				
		100	200	400	600	800
W	Clamped	0.4360	0.7923	1.3872	2.0182	2.8536
	Clamped -Simply supported	1.8741	3.7461	7.4844	11.216	14.940
$\Sigma_{rz}$	Clamped	0.2046	0.4081	0.7920	1.1204	1.3817
	Clamped -Simply supported	3.0036	5.9636	11.752	17.366	22.804

% Difference of  $(w_i) = 100 \times [(w_i)_{\text{Without. - app.}} - (w_i)_{\text{With. - app.}}] / (w_i)_{\text{Without. - app.}}$

% Difference of  $(\Sigma_{ij}) = 100 \times [(\Sigma_{ij})_{\text{With. - app.}} - (\Sigma_{ij})_{\text{Without. - app.}}] / (\Sigma_{ij})_{\text{With. - app.}}$

properties subjected to thermo-mechanical loading is presented. The problem is formulated based on the elasticity theory. The initial thermal stresses are obtained by solving the thermoelastic equilibrium

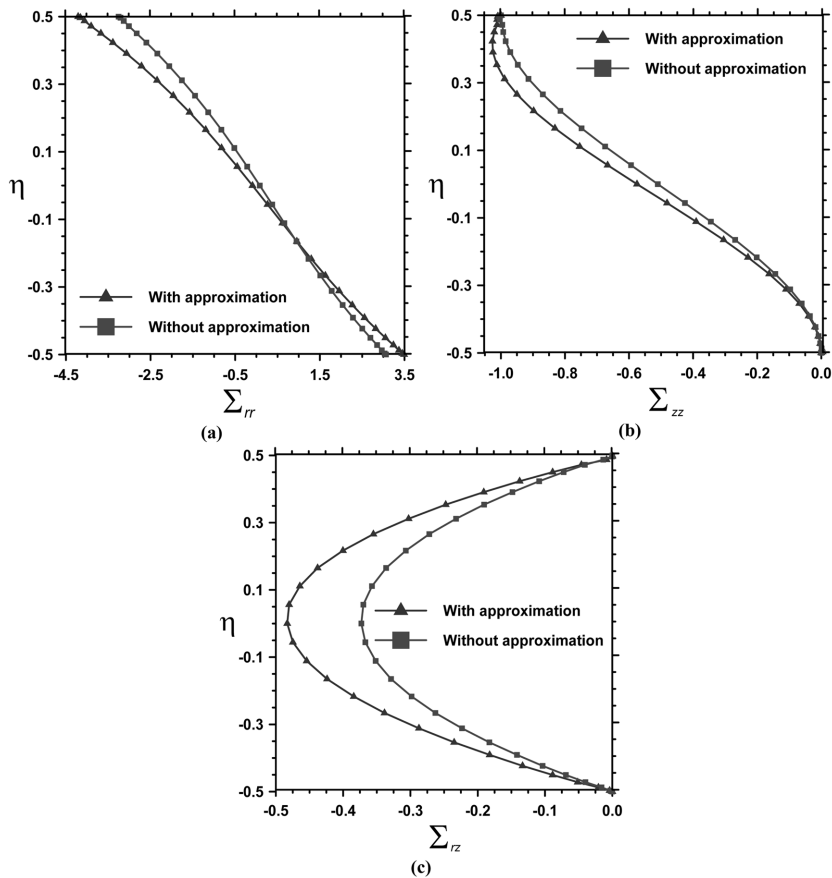


Fig. 6 (a)-(c) Comparison of the stresses of the clamped-simply supported FG annular plate with and without approximation of initial thermal stress ( $\lambda = 0.5, \xi = 0.5, p = 1, h/R_o = 0.2$ ).

Table 7 The non-dimensional the central deflection ( $-W$ ) of the FG annular plate subjected to thermal environment ( $\xi = 0.5, \eta = 0, p = 2, \Delta T = 800 K$ )

$h / R_o$	Uniform temperature rise				Non-Uniform temperature rise			
	$\lambda = 0.2$		$\lambda = 0.5$		$\lambda = 0.2$		$\lambda = 0.5$	
	C-C	C-S	C-C	C-S	C-C	C-S	C-C	C-S
0.05	1071.1	429.88	50.575	64.530	202.83	319.73	27.437	47.637
0.1	38.607	61.358	6.4142	10.126	23.089	44.372	4.1916	7.2663
0.2	6.3455	10.539	1.5452	2.1546	4.2062	7.4717	1.3427	1.5074
0.3	2.8880	4.4171	0.8204	1.0292	1.9316	3.0892	0.5501	0.7111
0.5	1.2951	1.7143	0.4009	0.4361	0.8686	1.1808	0.2716	0.3003

equations of the plate. Using the virtual work principle, the thermo-mechanical equilibrium equations and the related boundary conditions, which include the effects of initial thermal stresses, are derived. The differential quadrature method as an efficient and accurate numerical tool is used to solve the governing equations. The effects of temperature rise and the different geometrical parameters on the displacement and stress components of the FG plates are investigated. It is shown that the temperature-dependence of the material properties has significant effects on the results. Also, it is exhibited that the exact evaluation of the initial thermal stress is essential for an accurate bending analysis of FG plates. Although this work has not been considered analytically, it is not impossible and it can be performed and it's still open. The solutions can be used as benchmark for other numerical methods.

## References

- Reddy, J.N. and Cheng, Z.Q. (2001), "Three-dimensional thermomechanical deformations of functionally graded rectangular plates," *Eur. J. Mech. A Solids*, **20**(5), 841-855.
- Qian, L.F., Batra, R.C., and Chen, L.M. (2004), "Static and dynamic deformations of thick functionally graded elastic plates by using higher-order shear and normal deformable plate theory and meshless local Petrov-Galerkin method," *Compos Part B: Eng*, **35**(6-8), 685-697.
- Ferreira, A.J.M., Batra, R.C., Roque, C.M.C., Qian, L.F., and Pals, M. (2005), "Static analysis of functionally graded plates using third-order shear deformation theory and a meshless method," *Compos Struct*, **69**(4), 449-457.
- Reddy, J.N., Wang C.M., Kitipornchai S. (1999), "Axisymmetric bending of functionally graded circular and annular plates," *Euro J Mech A Solids*, **18**(2), 185-199.
- Cheng, Z.Q. and Batra, R.C. (2000), "Three-dimensional thermoelastic deformations of a functionally graded elliptic plate," *Compos Part B: Eng*, **31**(2), 97-106.
- Ma, L.S. and Wang, T.J. (2003), "Nonlinear bending and post-buckling of a functionally graded circular plate under mechanical and thermal loadings," *Int J Solids Struct*, **40**(13-14), 3311-30.
- Ma, L.S. and Wang, T.J. (2004), "Relationships between the solutions of axisymmetric bending and buckling of functionally graded circular plates based on the third-order plate theory and the classical solutions for isotropic circular plates," *Int J Solids Struct*, **41**(1), 85-101.
- Najafzadeh, M.M. and Heydari, H.R. (2004), "Thermal buckling of functionally graded circular plates based on higher order shear deformation plate theory," *European Journal of Mech.- A/Solids*, **23**(6), 1085-1100.
- Li, X.Y., Ding, H.J. and Chen, W.Q. (2008), "Three-dimensional analytical solution for functionally graded magneto-electro-elastic circular plates subjected to uniform load," *Compos Struct*, **83**(4), 381-390.
- Li, X.Y., Ding, H.J. and Chen, W.Q. (2008), "Elasticity solutions for a transversely isotropic functionally graded circular plate subject to an axisymmetric transverse load  $q^k m$ " *Int J Solids Struct*, **45**(1), 191-210.
- Saidi, A.R., Rasouli, A. and Sahraee, S. (2009), "Axisymmetric bending and buckling analysis of thick functionally graded

- circular plates using unconstrained third-order shear deformation plate theory,” *Compos Struct*, **89**(1), 110-119.
- Saidi, A.R. and Hasani Baferani, A. (2010), “Thermal buckling analysis of moderately thick functionally graded annular sector plates,” *Compos. Struct.*, **92**(7), 1744-1752.
- Sanjay Anandrao K., Gupta R.K., Ramchandran P. and Venkateswara Rao G. (2010), “Thermal post-buckling analysis of uniform slender functionally graded material beams,” *Struct. Eng. and Mech., An International Journal*, **36**, 5.
- Noda, N. (1991), “Thermal stresses in materials with temperature-dependent properties,” *Appl Mech Rev*, **44**(9), 383-397.
- Malekzadeh, P. (2009), “Two-dimensional in-plane free vibrations of functionally graded circular arches with temperature-dependent properties,” *Compos Struct*, **91**(1), 38-47.
- Malekzadeh, P. Shahpari, S.S. and Ziaee, H.R. (2010), “Three-dimensional free vibration of thick functionally graded annular plates in thermal environment,” *J Sound Vib*, **329**(4), 425-442.
- Bert, C.W and Malik, M. (1996), “Differential quadrature method in computational mechanics: A review,” *Appl Mech Rev*, **49**(1), 1-27.
- Malekzadeh, P. Golbahar Haghighi, M.R. and Atashi, M.M. (2010), “Out-of-plane free vibration of functionally graded circular curved beams in thermal environment,” *Compos Struct*, **92**(2), 541-552.
- Malekzadeh, P. Setoodeh, A.R. and Barmshouri, E. (2008). “A hybrid layerwise and differential quadrature method for in-plane free vibration of laminated thick circular arches,” *J Sound Vib*, **315**(1-2), 215-225.
- Kim, Y.W. (2005), “Temperature-dependent vibration analysis of functionally graded rectangular plates,” *J Sound Vib*, **284**(3-5), 531-549.
- Prakash, T. and Ganapathi, M. (2006), “Asymmetric flexural vibration and thermoelastic stability of FGM circular plates using finite element method,” *Compos Part B: Eng*, **37**(7-8), 642-649.
- Lanhe, W.U. (2004), “Thermal buckling of a simply supported moderately thick rectangular FGM plate,” *Composite Structures*, **64**(2), 211-218.